9496–9507 *Nucleic Acids Research, 2021, Vol. 49, No. 16* *Published online 17 August 2021*
https://doi.org/10.1093/nar/gkab699

Arabidopsis retains vertebrate-type telomerase accessory proteins via a plant-specific assembly

Jiarui Song[1], Claudia Castillo-González[1], Zeyang Ma[2,3] and Dorothy E. Shippen[1,*]

[1]Department of Biochemistry and Biophysics, Texas A&M University, College Station, TX 77843-2128, USA, [2]National Maize Improvement Center of China, China Agricultural University, 100193 Beijing, China and [3]College of Agronomy and Biotechnology, China Agricultural University, 100193 Beijing, China

Received May 17, 2021; Revised July 08, 2021; Editorial Decision July 29, 2021; Accepted August 11, 2021

ABSTRACT

The recent discovery of the bona-fide telomerase RNA (TR) from plants reveals conserved and unique secondary structure elements and the opportunity for new insight into the telomerase RNP. Here we examine how two highly conserved proteins previously implicated in Arabidopsis telomere maintenance, AtPOT1a and AtNAP57 (dyskerin), engage plant telomerase. We report that AtPOT1a associates with Arabidopsis telomerase via interaction with TERT. While loss of AtPOT1a does not impact AtTR stability, the templating domain is more accessible in *pot1a* mutants, supporting the conclusion that AtPOT1a stimulates telomerase activity but does not facilitate telomerase RNP assembly. We also show, that despite the absence of a canonical H/ACA binding motif within AtTR, dyskerin binds AtTR with high affinity and specificity *in vitro* via a plant specific three-way junction (TWJ). A core element of the TWJ is the P1a stem, which unites the 5′ and 3′ ends of AtTR. P1a is required for dyskerin-mediated stimulation of telomerase repeat addition processivity *in vitro*, and for AtTR accumulation and telomerase activity *in vivo*. The deployment of vertebrate-like accessory proteins and unique RNA structural elements by Arabidopsis telomerase provides a new platform for exploring telomerase biogenesis and evolution.

INTRODUCTION

The telomerase ribonucleoprotein (RNP) complex maintains telomere integrity and thus is a key invention enabling the transition from circular prokaryotic chromosomes to the linear chromosomes of eukaryotes (1). The essential core of telomerase consists of the catalytic telomerase reverse transcriptase (TERT) and a long noncoding RNA (TR/TER) (2). Telomerase RNA (TR) serves as a template for synthesis of telomere repeats by TERT. TR also provides a structural scaffold for accessory proteins that facilitate TR biogenesis, RNP assembly, engagement with the chromosome terminus and regulation of telomerase enzymatic activity (3).

Studies of TR secondary structure have revealed two domains essential for telomerase catalysis (4–6). The first is a template-pseudoknot domain bearing a single-stranded template, a double-stranded template boundary element and a pseudoknot (PK) motif (7–9). The second is a 'stem-terminus' element (STE) near the TR 3′ end termed helix IV in ciliates or CR4/5 in vertebrates (10–12). The template-PK and STE domains are sufficient to reconstitute telomerase activity in trans (4,6,12,13). The remainder of TR consists of diverse structural motifs that connect species-specific accessory proteins (14).

The composition of telomerase accessory factors is also highly divergent and reflects distinct modes of RNP biogenesis. In *Tetrahymena thermophila*, for example, the La-related protein P65 recognizes the 3′ poly-U tail of RNA Polymerase III (Pol III) transcribed TtTR and bends the RNA to promote telomerase RNP assembly (15–17). Recent cryo-EM analysis demonstrates the Tetrahymena enzyme also engages P75-P45-P19, a large RPA-like heterotrimer analogous to the telomere replication complex, CTC1/STN1/TEN1 (CST) (18). Unlike ciliate TR, fungal and vertebrate TR molecules are transcribed by RNA polymerase II (Pol II). The yeast TR (ScTER1 and SpTER1) require components of the snRNA biogenesis pathway for 3′ end maturation, resulting in RNP assembly with Sm and Lsm proteins (19,20). Interestingly, fission yeast telomerase associates with an additional La-related protein, Pof8, via a noncanonical interaction with the PK motif of SpTER1 (21–23). Vertebrate telomerase RNP biogenesis proceeds by yet another maturation pathway devised for small Cajal body RNAs (scaRNA) and small nucleolar RNAs (snoRNA) (24). Vertebrate TR associates with H/ACA snoRNP factors (dyskerin, NOP10, GAR1 and NHP2) as well as the Cajal body box (CAB box) binding protein TCAB (25–27). The dyskerin complex recognizes a conserved H/ACA motif that protects the 3′ end of the mature mammalian TR from exonuclease degra-

*To whom correspondence should be addressed. Tel: +1 979 862 2342; Fax: +1 979 862 7638; Email: dshippen@tamu.edu

dation (25,28). Cryo-EM studies of substrate-loaded human telomerase holoenzyme show a bilobed architecture consisting of the catalytic core (TERT and hTR) on one side, and a H/ACA RNP containing two sets of dyskerin-NOP10-GAR1-NHP2 tetramer on the other side (29,30). These observations highlight the remarkable diversity of telomerase accessory proteins and the co-evolution of the TR scaffold (31).

Analysis of telomerase in plants has lagged relative to other organisms. However, the bona-fide TR from *Arabidopsis thaliana* (AtTR) was recently identified using an unbiased approach for active telomerase purification (13) and independently, by a bioinformatics strategy (32). The two studies uncovered a total of approximately 100 AtTR orthologs spanning three major clades within the plant kingdom. Plant TR contains a 14-nt template region, including 7 nts dedicated to proper alignment of the telomeric 3′ terminus in the enzyme active site. Construction of a secondary structure model for plant TR revealed a conserved PK domain with a ciliate-like unstable stem and a vertebrate-like extensive single-stranded loop (13). Thus, the chimeric plant PK can be viewed as an 'evolutionary bridge' for the structural transition in highly divergent TR. Additional plant-specific RNA elements were distinguished, including the P1a stem, formed from a long-range interaction between the 5′ and 3′ ends of the RNA, and a flexible linker connecting P1b to P1c (13). These unique RNA elements have the potential to bind accessory proteins. Consistent with this notion, gel filtration chromatography of *A. thaliana* telomerase demonstrated that the core RNP is approximately 300 kDa in size (13), significantly larger than the 130 kDa TERT and 85 kDa AtTR. Uncovering the accessory factors of plant telomerase may be particularly informative as plant TR is transcribed by Pol III transcript, unlike its counterparts in yeast and vertebrates (32,33).

POT1 (Protection of Telomeres) is a leading candidate for a telomerase accessory factor in Arabidopsis. One of the most conserved constituents of the telomere complex (34), POT1 harbors oligosaccharide/oligonucleotide-binding folds (OB-fold) that facilitate interaction with single-stranded telomeric DNA (35). Human POT1 is a stable component of telomeres and a core component of the shelterin complex (36,37). Bridging by its binding partner TPP1, hPOT1 engages telomerase through the highly conserved TEN domain within TERT (38). hPOT1-TPP1 dynamically regulates telomere length homeostasis with diverse roles in protecting the telomere ssDNA from degradation and repair (39,40), inhibiting telomerase activity (41,42), and reducing the primer dissociation rate to promote telomerase repeat addition processivity (RAP) (43,44).

Arabidopsis thaliana encodes two POT1 paralogs, POT1a and POT1b (45–47). AtPOT1a exhibits both conserved and unique functions relative to hPOT1. Unlike hPOT1, AtPOT1a is not a stable component of telomeric chromatin and it is not required to recruit TERT to telomeres *in vivo* (48,49). However, similar to hPOT1-TPP1 complex, AtPOT1a can bind telomeric DNA, stimulate telomerase RAP *in vitro* (50) and is required for telomere maintenance *in vivo* (45,48). Considering that AtPOT1a also associates with enzymatically active telomerase (48), the data argue that AtPOT1a functions as a telomerase accessory factor rather than a shelterin component. How AtPOT1a engages telomerase and stimulates its activity is unknown.

Another potential subunit of plant telomerase is dyskerin (*NAP57*). Dyskerin is reported to associate with enzymatically active telomerase in both eudicots *(A. thaliana)* and monocots (*Allium cepa)* (32,51). Although a homozygous null mutation in *AtNAP57* is lethal (51,52), transgenic Arabidopsis carrying a single wild type *AtNAP57* allele with a second allele bearing a T66A mutation are viable. Such plants exhibit decreased telomerase activity and defective telomere maintenance (51), indicating that dyskerin is critical for telomerase function. Strikingly, plant TR does not harbor the canonical H/ACA motif essential for anchoring dyskerin to vertebrate TR (13). Thus, it is unclear how dyskerin associates with plant telomerase.

Here, we examine the interactions of AtPOT1a and dyskerin with the Arabidopsis telomerase RNP. We show that AtPOT1a physically interacts with TERT in an AtTR-independent manner. However, loss of AtPOT1a increases accessibility of the AtTR templating domain *in vivo,* supporting the conclusion that AtPOT1a stimulates telomerase activity, but does not facilitate telomerase RNP assembly. In contrast to AtPOT1a, we report a direct interaction between dyskerin and AtTR via a plant-specific three-way junction within AtTR, which includes a novel P1a stem. Disruption of P1a prevents dyskerin-mediated stimulation of telomerase RAP *in vitro*, and blocks AtTR accumulation and telomerase activity *in vivo*. These findings indicate that the plant telomerase represents a chimeric RNP, harboring a ciliate-like Pol III transcribed TR with unique structural elements that assembles with vertebrate-like accessory proteins.

MATERIALS AND METHODS

Plant material, growth conditions and transformation

Arabidopsis thaliana accession Col-0, WS, *attr* (Flag_410H04) (13), *attert* (SALK_041265C) (53) and *atpot1a* (48) were used in this study. Seeds were sterilized in 50% bleach with 0.1% Triton X-100 and then plated on half Murashige and Skoog (half MS) medium with 0.8% agar. Plants were grown at 22°C under long day light conditions. For genetic complementation, pHSN6A01-AtTR, pHSN6A01-m16, pHSN6A01-m17 and pHSN6A01-m18 were transformed into second generation *AtTR*-/- (Flag_410H04) plants using Agrobacterium-mediated (*A. tumefasciens* GV3101) transformation as described (54). Transformants were selected on hygromycin in T1 and analyzed for telomerase phenotypes. In parallel, untransformed *AtTR*+/+ and *AtTR*-/- plants were analyzed.

Plasmids

DNA sequences that encode full-length dyskerin (AtNAP57) (residues 1–565) or dyskerin$_{\Delta C}$ (residues 1–439) were cloned into a kanamycin-resistant pET28a plasmid to achieve a N-terminal 6xHis tag using the NEBuilder HiFi DNA assembly cloning kit. For co-expression of dyskerin$_{\Delta C}$-NOP10-GAL1$_{53\text{-}145}$, coding sequences of

dyskerin$_{\Delta C}$ and full-length NOP10 (residues 1–64) were cloned into an ampicillin-resistant pETDuet-1 plasmid to occupy independent expression cassettes using the NEBuilder HiFi DNA assembly cloning kit. Dyskerin$_{\Delta C}$, but not NOP10, was fused with a N-terminal 6xHis tag. GAL1$_{53\text{-}145}$ (AT3G03920) (residues 53–145) was cloned separately into a kanamycin-resistant pET28a plasmid without any tag fused to its N- or C-terminus. For genetic complementation, *AtTR* was cloned into a binary vector pHSN6A01 under the control of the U6 promoter using the NEBuilder HiFi DNA assembly cloning kit. Mutagenesis was applied to pHSN6A01-AtTR to produce 18 AtTR variants using the Q5 site-directed mutagenesis kit (NEB). For *in vitro* co-IP and telomerase reconstitution assays, full-length *AtPOT1a* coding sequence was cloned into a pET28a plasmid to allow attachment with an N-terminal T7 tag. The pCITE-3xFLAG-AtTERT plasmid was a generous gift from Dr. Julian J.-L. Chen (Arizona State University).

Protein expression and purification

All proteins were expressed in *Escherichia coli* Rosetta (DE3) strains that provide additional tRNAs. For purification of individual full-length dyskerin or dyskerin$_{\Delta C}$ protein, cells were resuspended in 50 mM Tris-Cl pH 7.3, 400 mM NaCl, 5% glycerol, and 2 mM DTT and lysed by a microfluidizer. Proteins were purified through HisTrap-HP column (GE Healthcare) and Superdex 200 increase 10/300 gel filtration chromatography (GE Healthcare). For reassembly and purification of dyskerin$_{\Delta C}$-NOP10-GAL1$_{53\text{-}145,}$ the heterotrimer was co-expressed from a pETDuet-1 plasmid expressing dyskerin$_{\Delta C}$ and Nop10 and a pET28a plasmid expressing GAL1$_{53\text{-}145}$. The complex was purified through a HisTrap-HP column (GE Healthcare) and Superdex 200 Increase 10/300 gel filtration chromatography (GE Healthcare) in buffer (50 mM Tris-Cl pH 7.3, 350 mM KCl and 2 mM DTT). An additional 5 mM DTT was provided before storage at -80°C.

RIP and co-IP

Anti-AtTERT antibody was affinity-purified as previously described (13). Briefly, antibody was preincubated with protein A magnetic beads (Dynabeads) at 4°C for 2 h before IP. About 1.5 g of WT (Col-0) Arabidopsis seedlings were ground in liquid nitrogen and homogenized in RIP buffer (100 mM Tris-OAC pH 7.5, 150 mM KGlu, 1 mM $MgCl_2$, 0.5% Triton X-100, 0.1% Tween 20, 20 μl/ml Plant protease inhibitor mixture [Sigma-Aldrich], 1 μl/ml RNaseOUT [Thermo Fisher Scientific] and 2.5 mM DTT). After clearing by centrifugation, protein complexes were immunoprecipitated using preincubated anti-AtTERT magnetic beads at 4°C for 3 h. After incubation, beads were washed seven times with RIP buffer and then resuspended with 1 ml of TRIzol reagent (Invitrogen) to extract RNA. For the TRAP measurement of IP samples, prior to resuspending in TRIzol, 5% beads were transferred into TRAP extension reaction (50 mM Tris-Cl pH 8.0, 50 mM KCl, 2 mM DTT, 3 mM $MgCl_2$, 1 mM spermidine, 1 μM TRAP-F primer, and 0.5 mM each ddNTPs) and incubated at 30°C for 45 min. Extended products were ethanol precipitated and used for direct TRAP assay as described (13).

For *in vitro* co-immunoprecipitation experiments, co-expression of T7-AtPOT1a and 3xFLAG-AtTERT was conducted using a TNT Quick Coupled transcription/translation kit (Promega) following the manufacturer's instructions with ^{35}S-methionine labeling. *In vitro* folded AtTR, non-specific RNA (yeast tRNA) or mock (water) was provided independently into the respective reactions. *In vitro* reconstituted complexes were immunopurified with anti-FLAG M2 magnetic beads (Sigma-Aldrich) at room temperature for 1.5 h to enrich AtTERT and copurified proteins. The products were resolved on a 10% SDS-PAGE gel, dried, exposed and detected by a Typhoon FLA 9500 phosphorimager (GE Healthcare).

For *in vivo* co-IP, 1.5 g of wild-type (WT) (WS accession) or *attr* seedlings were ground in liquid nitrogen and homogenized in co-IP buffer (100 mM Tris-OAC pH 7.5, 150 mM KGlu, 1 mM $MgCl_2$, 0.5% Triton X-100, 0.1% Tween 20, 20 μl/ml Plant protease inhibitor mixture [Sigma-Aldrich], 1 μl/ml RNaseOUT [Thermo Fisher Scientific] and 2.5 mM DTT). After clearing by centrifugation, protein complexes were immunoprecipitated using preincubated anti-AtTERT magnetic beads at 4°C for 3 h. After incubation, beads were washed seven times with co-IP buffer and then resuspended in SDS-loading buffer. Copurified proteins were resolved on an 8% SDS-PAGE gel and analyzed by western blot.

Antisense LNA oligo pull down

An antisense LNA oligo pull-down assay was adapted from (55,56) with modifications. Two antisense LNA oligos were designed to target the accessible regions within AtTR and labeled with Biotin at the 3′ end. About 2 g of formaldehyde-crosslinked four-day-old WT (WS) or *attr* seedlings were homogenized in lysis buffer (50 mM Tris-OAC pH 7.5, 10 mM EDTA, 1% SDS, 20 μl/ml Plant protease inhibitor mixture [Sigma-Aldrich], 1 μl/ml RNaseOUT [Thermo Fisher Scientific] and 6 mM DTT). The pre-warmed 2× hybridization buffer (50 mM Tris-OAC pH 7.5, 750 mM NaCl, 15% formamide, 1 mM EDTA, 20 μl/ml Plant protease inhibitor mixture [Sigma-Aldrich], 1 μl/ml RNaseOUT [Thermo Fisher Scientific] and 6 mM DTT) and 100 pmol antisense LNA oligos were incubated at 42°C for 2 h to achieve oligo annealing. About 100 μl Dynabeads MyOne Streptavidin C1 beads (Thermo Fisher Scientific) was added and incubated for additional 45 min at 42°C. Beads were washed five times with wash buffer (2× SSC, 0.5% SDS, 1 mM PMSF, 5 mM DTT) before resuspending 90% of beads in SDS-loading buffer for protein analysis by western blot. The remaining 10% of beads was subjected to protease K digestion (10 mM Tris-Cl pH 7, 100 mM NaCl, 1 mM EDTA, 0.5% SDS and 5% 20 mg/ml protease K) at 50°C for 45 min prior to the RNA extraction by TRIzol reagent. The extracted RNA was analyzed by RT-qPCR for RNA abundance.

Target-specific DMS-MaPseq

The DMS-MaPseq assay was adapted from (57) and performed as described (13). Briefly, 4-day-old WT (Col-0) or *atpot1a* seedlings were treated with 1% DMS or water

(mock samples) in DMS reaction buffer (40 mM HEPES pH 7.5, 100 mM KCl and 0.5 mM $MgCl_2$) with two times of 7.5 min vacuum. Total RNA was extracted from respective samples using RNA Clean & Concentrator-5 (Zymo Research) including in-column DNase digestion. About 5 μg of high-quality RNA combined with gene-specific primers (AtTR or ACT2 mRNA) (5 pmol each) was heated and annealed for primer binding. TGIRT (Ingex) reaction was assembled following manufacturer's instructions. After RT, 1 μl of cDNA solution was directly added into a 50-μl PCR reaction using Phusion High-Fidelity DNA Polymerase (New England BioLabs) to amply AtTR or ACT2 mRNA. PCR products were gel-purified, quantified and directly assembled into Illumina sequencing libraries using the NEBNext Ultra II DNA Library Prep Kit (NEB) with 25 ng input. One mock library and two DMS libraries were built for each sample. Sequencing was performed on an 150 × 2 Illumina NextSeq 500 platform at Texas A&M University.

EMSA

EMSA was adapted from (50) with modifications. WT AtTR and AtTR variants were prepared with an AmpliScribe T7-Flash transcription kit and purified by 6% denaturing PAGE. Purified RNAs were 5′ end labeled with ^{32}P-ATP (Perkin Elmer) using T4 Polynucleotide kinase (NEB) and PAGE purified again to remove free ATP. Radiolabeled RNAs or non-radiolabeled competitors were folded by heating at 98°C for 2 min and slow cooling to room temperature. Full-length dyskerin or dyskerinΔC protein was diluted and mixed with RNA in EMSA reaction (25 mM Tris-Cl pH 7.5, 50 mM KCl, 2 mM $MgCl_2$, 10% glycerol, 1 mM DTT, 50 μg/ml BSA, 50 μg/ml yeast tRNA and 1 μl/ 20 μl RNaseOUT [Thermo Fisher Scientific]) at 30°C for 30 min. EMSA products were separated on 5% native PAGE in glycine buffer pH 9.0 at 4°C. Gels were dried under vacuum at 80°C for 1 h prior to exposure to a phosphor imager screen. Data were collected on Typhoon FLA 9500 phosphorimager (GE Healthcare) and quantified using Quantity One software (Bio-Rad).

In vitro telomerase reconstitution and TRAP

In vitro telomerase reconstitution was performed as described (13,58) with modifications. Briefly, 3xFLAG-AtTERT was expressed in rabbit reticulocyte lysate (RRL) (TNT Quick Coupled transcription/translation kit; Promega) following the manufacturer's instructions. WT AtTR or AtTR variants were *in vitro* transcribed, folded, and assembled with AtTERT in RRL for 20 min at 30°C at a final concentration of 1.5 μM (13,58). Serial dilutions of full-length dyskerin or $Dyskerin_{\Delta C}$-NOP10-$GAL1_{53\text{-}145}$ heterotrimer were added to the TERT-AtTR RRL mixture and incubated for an additional 20 min. Reconstituted telomerase was immunopurified with anti-FLAG M2 magnetic beads (Sigma-Aldrich) at room temperature for 1 h. On-beads telomerase was measured for telomerase activity via direct primer extension assay as described (13,58). Briefly, beads were resuspended in a reaction containing telomerase reaction buffer (50 mM Tris-Cl pH 8.0, 50 mM NaCl, 0.5 mM $MgCl_2$, 2 mM DTT and 1 mM spermidine), 1 μM extension primer, ddNTPs and 0.18 μM of ^{32}P-dGTP (PerkinElmer). Reactions were incubated at 30°C for 90 min and terminated by phenol/chloroform extraction, followed by ethanol precipitation. A radiolabeled recovery control was mixed with each reaction before phenol/chloroform extraction. DNA products were resolved by 10% denaturing PAGE gel, dried, exposed and imaged on a Typhoon FLA 9500 phosphorimager (GE Healthcare). Signal intensities were quantified using Quantity One software (Bio-Rad).

The TRAP assay was conducted as described (50) with modifications. Unopened Arabidopsis flower bundles were collected for partial purification of telomerase. Purified telomerase was mixed in Go Taq Master Mix (Promega) containing a TRAP forward primer and incubated for 30 min at room temperature. After extension, 0.4 μM reverse primer was added to the reaction followed by 20 PCR cycles. Products were resolved by 6% denaturing PAGE, dried, exposed and imaged on Typhoon FLA 9500 phosphorimager (GE Healthcare).

qRT-PCR

qRT-PCR was performed as described (59) with modifications. Briefly, Arabidopsis flower bundles or 6-day old seedlings were collected for RNA extraction using the Direct-zol RNA kit (Zymo Research). cDNA synthesis was conducted using SuperScript IV reverse transcriptase (Invitrogen) and random primer mix (NEB). cDNA was diluted and added into PowerUp SyBr Green for qPCR reactions with the corresponding primers provided in the Supplementary Table S1.

RESULTS

AtPOT1a engages telomerase via an AtTR-independent mechanism

To test whether AtPOT1a assembles into the same RNP complex with AtTR, we employed RNA immunoprecipitation (RIP) with polyclonal anti-AtPOT1a and anti-AtTERT antibodies (Figure 1A, left). As expected, telomerase activity was enriched in both the AtPOT1a and TERT IP samples but not with the GFP IP control (Figure 1A, right). Moreover, qPCR showed that the TERT and AtPOT1a IP significantly enriched AtTR but not GAPDH mRNA. Next, we asked if AtPOT1a played a role in promoting AtTR stability by measuring the steady state level of AtTR in a *pot1a* homozygous T-DNA insertion mutant (48) (Figure 1B). There was no difference in AtTR abundance in *pot1a* mutants versus wild-type plants, indicating that AtPOT1a is not required for AtTR biogenesis. Interestingly, the abundance of AtTR was also not changed in *tert* knockout mutants (53) (Figure 1B), suggesting that other factors besides TERT and AtPOT1a are necessary for AtTR biogenesis and/or stability.

While TR acts as a framework for many telomerase accessory factors (60), some proteins directly interact with TERT, including the human POT1-TPP1 heterodimer and the P75-P45-P19 complex in Tetrahymena (18,43). We employed co-IP experiments with recombinant FLAG-tagged TERT and T7-tagged AtPOT1a to test if these proteins interact with

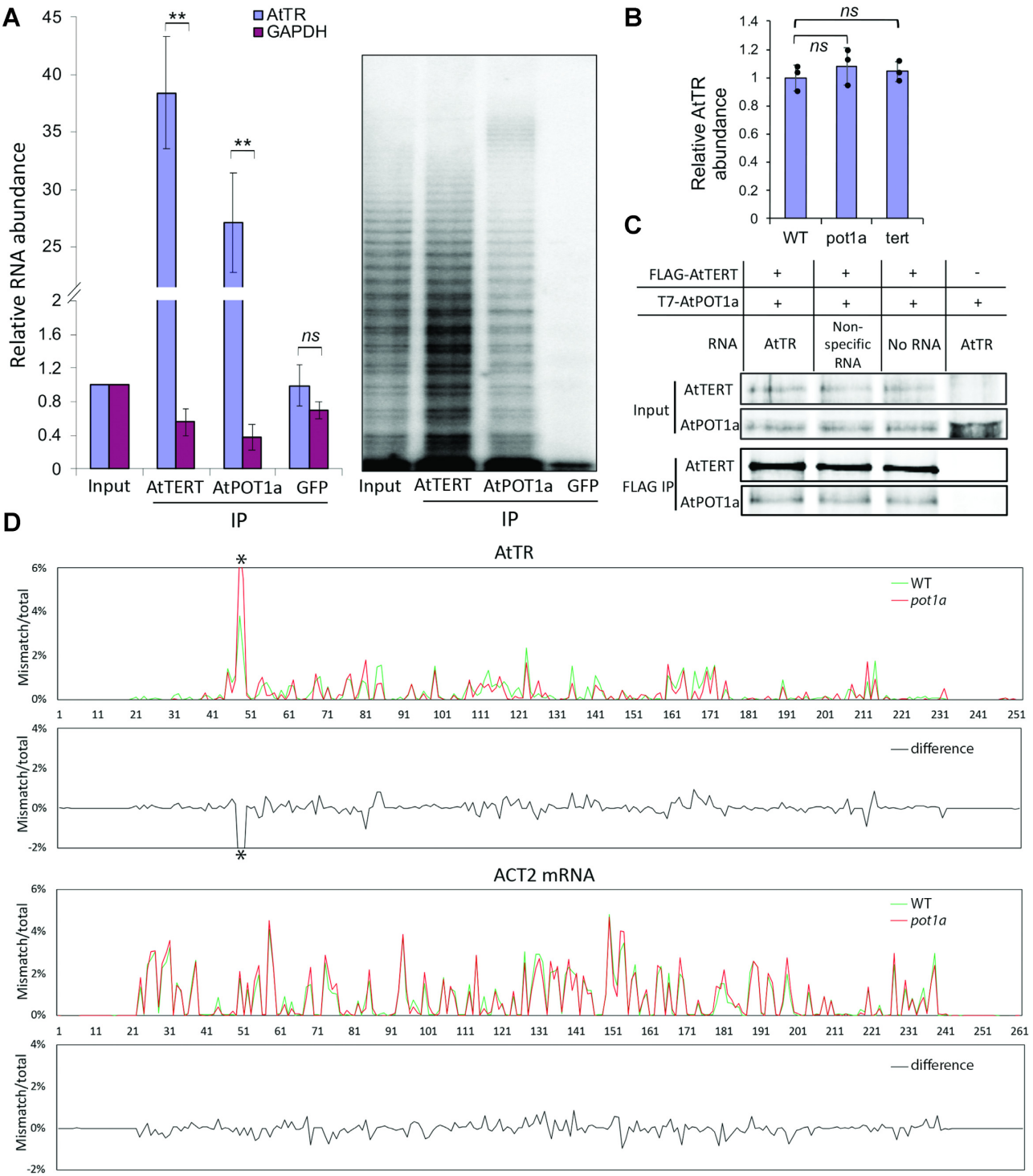

Figure 1. AtPOT1a does not engage Arabidopsis telomerase via interaction with AtTR. (**A**), qPCR (left) and TRAP (right) results from immunoprecipitated samples to measure the copurification of AtTR (left), GAPDH mRNA (left) and active telomerase (right). Anti-AtTERT and Anti-GFP IPs served as positive and negative controls, respectively. Error bars indicate standard deviation. $^{**}P$ value < 0.01 and *ns* (not significant) were calculated based on Student's *t*-test. (**B**) qPCR results for AtTR in wild-type (WT), *tert* and *pot1a* mutants. A single data point represents an individual biological repeat. Error bars indicate standard deviation. *ns* was calculated based on Student's *t*-test. (**C**) *In vitro* co-IP experiments performed in a coupled transcription/translation system in the presence or absence of different RNA molecules. Co-purification of AtPOT1a was measured after Anti-FLAG IP. (**D**) *In vivo* chemical probing of RNA secondary structure by targeting specific DMS-MaPseq from WT Arabidopsis and *pot1a* mutants. Average mutation frequencies from two biological replicants are plotted along AtTR and ACT2 mRNA sequences separately. Asterisk (*) denotes the template region of AtTR with increased flexibility in the *pot1a* mutant.

each other *in vitro*, and if this interaction is dependent on AtTR. TERT and AtPOT1a constructs were expressed in rabbit reticulocyte (RRL) extract, and pull-down was performed using FLAG antibody followed by western blotting with T7 antibody. Detection of AtPOT1a indicated that AtPOT1a directly interacts with TERT (Figure 1C). Notably, the equivalent amount of AtPOT1a copurified in the presence of AtTR, in the presence of non-specific RNA, or in the absence of any RNA. We conclude that AtPOT1a physically associates with TERT and this interaction is not dependent on AtTR. This result is consistent with previous yeast two-hybrid and bimolecular fluorescence complementation data showing an interaction between AtPOT1a and the N-terminus of TERT (46,61).

To further explore the interaction of AtPOT1a with telomerase, we asked if AtPOT1a impacts AtTR structure and nucleotide accessibility *in vivo* using a DMS-MaPseq assay in wild-type and plants lacking AtPOT1a (Figure 1D and Supplementary Figure S1). The DMS-induced mismatch rate correlates with the respective flexibility and accessibility of individual A and C residues (62). Results of DMS-MaPseq were validated by plotting average mutation frequencies on the AtTR secondary structure (Supplementary Figure S1B and C). We observed no significant difference in nucleotide accessibility between wild-type and *pot1a* mutants for most of AtTR. However, there was a dramatic difference in accessibility of nucleotides C48 and C49, which are embedded in the alignment region of the TR template (Figure 1D). In the absence of AtPOT1a these residues were much more accessible in AtTR. The increase in TR template accessibility is consistent with inefficient interaction of telomerase with telomeric DNA in plants lacking AtPOT1a. Altogether, these findings indicate that AtPOT1a is not required for telomerase RNP assembly, but rather functions to stimulate telomerase interaction with telomeric DNA.

Dyskerin tightly binds AtTR and promotes telomerase RAP *in vitro*

Since prior biochemical and genetic experiments indicated that dyskerin (NAP57) associates with enzymatically active telomerase (32,51), we asked if this association is mediated by AtTR using two independent approaches. First, an *in vivo* co-IP experiment was conducted using anti-TERT antibody in wild-type and *attr* null mutants (Figure 2A). Dyskerin, the positive control TERT, and the negative control PEPC were detected by western blotting. Dyskerin copurified with TERT in extracts from wild-type plants, but not from mutants lacking AtTR. As a parallel strategy, we performed a pull-down using two antisense locked nucleic acid (LNA) oligonucleotides to capture proteins that directly bind AtTR (Figure 2B and C). The oligonucleotides were designed to target accessible regions within AtTR (13) (Supplementary Figure S2A). qPCR analysis of the pull-down samples showed a strong enrichment of AtTR, but not the ACT2 mRNA and GAPDH mRNA controls (Figure 2C and Supplementary Figure S2B), confirming the specificity of antisense LNA oligonucleotides. Western blotting revealed a background signal for dyskerin in the *attr* control reaction (Figure 2B). However, both dyskerin and TERT were highly enriched from the pull-down in wild-type plants. These results argue that ATR associates with dyskerin *in vivo* and this interaction facilitates dyskerin association with the telomerase enzyme.

We next examined the dyskerin-AtTR interaction *in vitro* using recombinant dyskerin protein. When expressed in *Escherichia coli*, full-length dyskerin formed aggregates, but this can be mitigated in a low concentration (Supplementary Figure S3A). To increase soluble protein yield, we removed the C-terminal disordered region (residues 440–565), which is predicted to contain a nuclear location signal (NLS) (Supplementary Figure S3C). Dyskerin$_{\Delta C}$ vastly enhanced protein solubility (Supplementary Figure S3B). Electrophoretic mobility shift assay (EMSA) was then used to monitor dyskerin$_{\Delta C}$-AtTR interaction (Figure 2D). A reliable signal from dyskerin$_{\Delta C}$-AtTR complex was observed after titration of 12.5 nM dyskerin$_{\Delta C}$ protein with radiolabeled AtTR, consistent with a stable dyskerin-AtTR complex. A 100-fold excess of specific, non-radiolabeled competitor, but not non-specific yeast tRNA, resolved the dyskerin$_{\Delta C}$-AtTR complex into free AtTR (Figure 2D, lanes 9–10). Quantification of EMSA with plots fit to the Hill equation revealed a dissociation constant (K_d) of 56 (±5) nM (Figure 2E), indicating a specific, high-affinity interaction between Dyskerin$_{\Delta C}$ and AtTR.

We next asked whether dyskerin could influence telomerase enzyme activity or repeat addition processivity (RAP) in an *in vitro* telomerase reconstitution assay (13). We were reluctant to use Dyskerin$_{\Delta C}$ in these experiments because of the potential loss of function with this truncated isoform. Therefore, different concentrations of Dyskerin$_{FL}$ were added to reactions containing RRL-expressed 3XFLAG-AtTERT and *in vitro* folded AtTR. Using a direct telomerase extension assay, we saw a substantial increase in signal intensity for high molecular weight products (+20, +27 and + 34) relative to shorter products (+6), suggesting that telomerase RAP is stimulated by the addition of dyskerin (Figure 2F). While the overall activity of the reaction containing 200 nM dyskerin$_{FL}$ was diminished, perhaps as a consequence of dyskerin aggregation, the length of telomerase products was proportional to the amount of dyskerin in the reaction (Figure 2F, lane 7). These findings verify that dyskerin physically interacts with AtTR and demonstrate that this interaction stimulates telomerase RAP *in vitro*.

The plant-specific P1a stem is required for dyskerin interaction with AtTR

Using competitive EMSA with recombinant Dyskerin$_{\Delta C}$ protein, we screened 15 AtTR truncation constructs to define RNA element(s) necessary for dyskerin association (Figure 3). Truncation constructs were designed by deleting different RNA motifs defined in the AtTR secondary structure model (Figure 3A). Strikingly, removing the P1a stem abolished Dyskerin$_{\Delta C}$ binding (construct 1). In contrast, truncation of the non-conserved distal stem-loop of STE (construct 2), the single-stranded linker connecting P1b to P1c (construct 3), the template region and stem P2.1

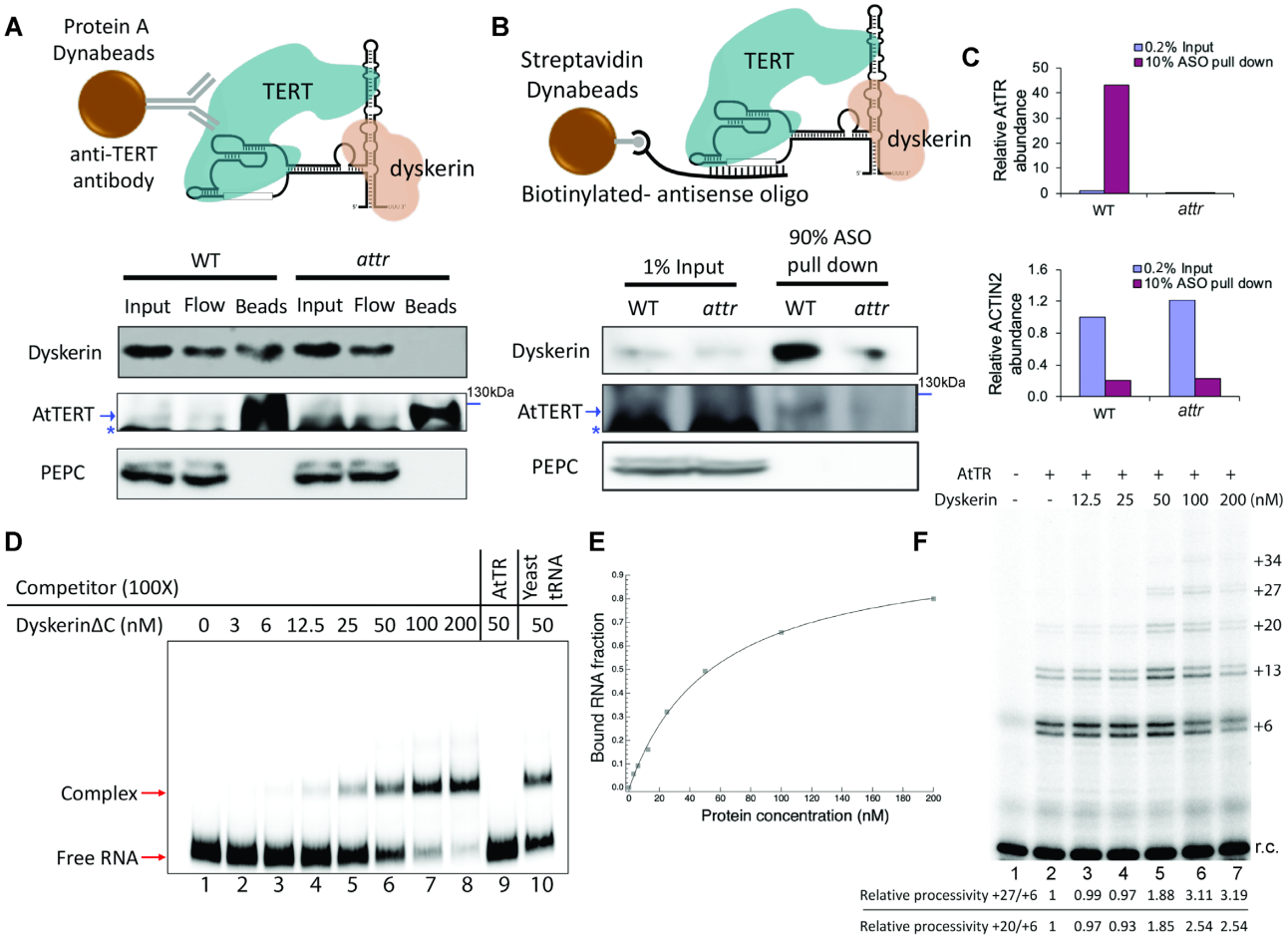

Figure 2. Dyskerin physically associates with AtTR and stimulates telomerase processivity *in vitro*. (**A**) Top: Schematic representation of *in vivo* co-IP experiment performed under native conditions. Bottom: Western blot analysis of dyskerin, AtTERT and PEPC in corresponding fractions. (**B**) Top: Schematic representation of the antisense LNA oligo pull down experiment performed after crosslinking. Bottom: Western blot analysis of dyskerin, AtTERT and PEPC in corresponding fractions. For panels (A and B), asterisk denotes a non-specific band detected by polyclonal anti-AtTERT antibody. Arrow indicates the expected AtTERT signal consistent with the molecular weight marker. (**C**) qPCR analysis of AtTR and ACT2 mRNA abundance in the antisense LNA oligo pull down. (**D**) EMSA to examine the dyskerinΔC-AtTR interaction *in vitro*. 100× specific (AtTR) or non-specific (yeast tRNA) competitors was provided to test binding specificity. (**E**) Quantification of EMSA results plotted and fitted to the Hill Equation with the Hill coefficient as 1. Bound RNA was calculated using the ratio of RNP signal intensity to total signal intensity. (**F**) *In vitro* telomerase reconstitution assay with a titration of $dyskerin_{FL}$ protein. Relative telomerase processivity is indicated at the bottom of the panel. A radiolabeled 18-mer recovery control (r.c.) was added before product purification and precipitation. This experiment was independently reproduced twice with identical results.

(construct 4), and two conserved single-stranded loops within P4 and P5 (constructs 10 and 11) did not impede the interaction (Figure 3B).

Connecting P1a to P1b and P4-P5-P6 generates a unique three-way junction (TWJ) structure (Figure 3A). To assess the importance of the TWJ, we removed P1a together with P4-P5-P6 (construct 5). Consistent with construct 1, construct 5 did not compete with full-length AtTR for $Dyskerin_{\Delta C}$ binding. We also found little competition in reactions with constructs 13, 14 and 15, indicating the importance of maintaining a complete PK structure for dyskerin association. One caveat with these experiments is that the constructs contained multiple modifications, which could impact the overall structure of AtTR. Nonetheless, our results imply that the plant-specific TWJ, including the unique P1a stem, is essential for dyskerin interaction with AtTR *in vitro*.

The P1a stem is essential for dyskerin-mediated stimulation of telomerase RAP *in vitro* and AtTR accumulation *in vivo*

In vertebrates and yeast, dyskerin associates with NOP10, GAL1, NHP2 and a target RNA subunit to assemble into a H/ACA RNP complex (63,64). Since our initial experiments employed only the dyskerin subunit, the absence of interaction partners could explain the low solubility of recombinant dyskerin protein. To obtain a more stable complex, we co-expressed three protein subunits of the plant H/ACA complex including $Dyskerin_{\Delta C}$, NOP10 and a truncation of GAL1 (residues 53–145; $GAL1_{53\text{-}145}$) in *E. coli* (Supplementary Figure S4). A similar complex is sufficient to reconstitute the functional yeast H/ACA complex (64). Notably, co-expression of NOP10 and $GAL1_{53\text{-}145}$ with $dyskerin_{\Delta C}$ significantly enhanced complex stability and solubility, allowing us to purify the $dyskerin_{\Delta C}$-NOP10-$GAL1_{53\text{-}145}$ heterotrimer (Supplementary Figure S4C).

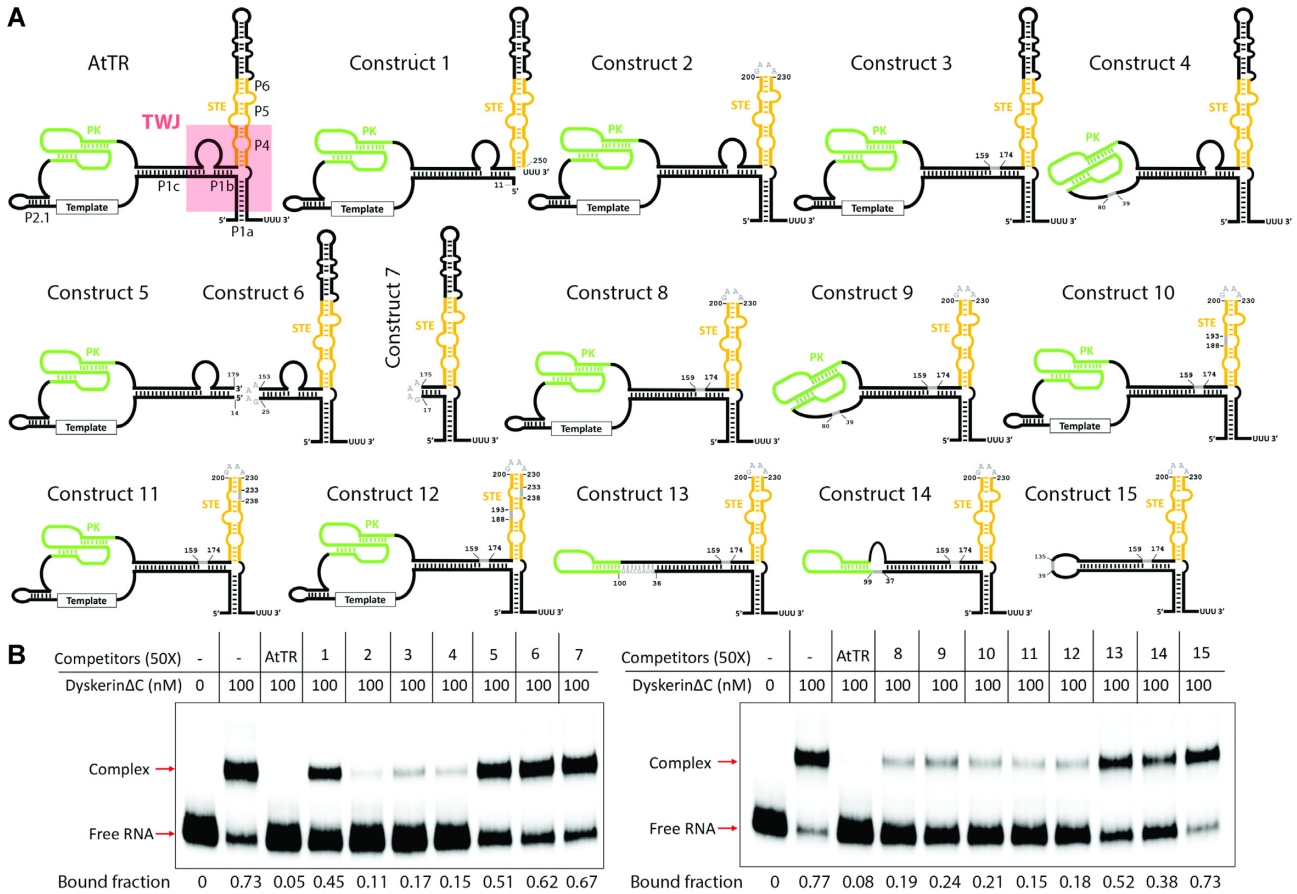

Figure 3. Mapping the dyskerin binding site on AtTR. (**A**) Secondary structures of WT AtTR and constructs 1–15. (**B**) Competitive EMSA performed with 50X excess non-radiolabeled AtTR or individual truncations. Signal intensities were quantified to calculate the bound RNA fraction. Mutation constructs 2, 3, 4, 8, 9, 10, 11 and 12 show strong competition; construct 14 shows moderate competition; constructs 1, 5, 6, 7, 13 and 15 show weak competition or no competition.

We used the recombinant heterotrimer complex to assess the impact on telomerase RAP reconstituted *in vitro* (Figure 4A and B). Consistent with the Dyskerin$_{FL}$ results, longer extension products (+20, +27, and + 34) were more abundant in the presence of the Dyskerin$_{\Delta C}$ complex (Figure 4B, lanes 2–4). We next asked if the P1a element, necessary for dyskerin association with AtTR, is required for telomerase stimulation *in vitro*. Telomerase reconstitution conducted with AtTR truncation construct 1 did not dramatically decrease enzyme activity and RAP relative to wild-type AtTR (Figure 4B, lanes 2 and 5). Strikingly, however, the Dyskerin$_{\Delta C}$ complex was unable to stimulate RAP with this AtTR variant (Figure 4B, lanes 5–7), indicating that P1a is required for dyskerin-mediated stimulation of telomerase RAP *in vitro*.

We used genetic complementation to examine the function of the P1a stem *in vivo*. *attr* null mutants were transformed with constructs containing U6 promoter-driven AtTR composed of either wild-type sequence (U6::AtTR) or one of three P1a variants: a non-complementary strand on the 5′ side of P1a (U6::m16), a non-complementary strand on the 3′ side of P1a (U6::m17) or a P1a stem with compensatory mutations, but similar structure to wild-type AtTR (U6::m18) (Figure 4C). Notably, the same canonical Pol III polyU terminator was applied to all of the constructs. Although expression of all four constructs was driven by the same U6 promoter and terminator, perturbation of P1a dramatically decreased the steady state level of U6::m16 and U6::m17 RNAs relative to U6::AtTR (Figure 4D). In marked contrast, U6::m18 reached the same level as U6::AtTR, implying that the architecture of the P1a stem was of paramount importance for AtTR biogenesis. Telomere repeat amplification protocol (TRAP) was performed to measure telomerase activity in these transgenic lines. Consistent with AtTR abundance, plants expressing U6::m16 and U6::17, but not U6::m18, displayed a significant reduction in telomerase activity compared to wild-type (Figure 4E). Hence, preserving the plant-specific P1a is not only critical for dyskerin-AtTR interaction *in vitro*, but disruption of P1a severely compromises AtTR and telomerase activity *in vivo*.

DISCUSSION

Telomere maintenance by telomerase is a near universal mechanism in eukaryotes, and yet TR and many accessory proteins exhibit dramatic divergence across different lineages (3,14). The recent discovery of TR from plants (13,32) fills an important gap in the evolutionary history of TR and provides a new opportunity for exploring different modes

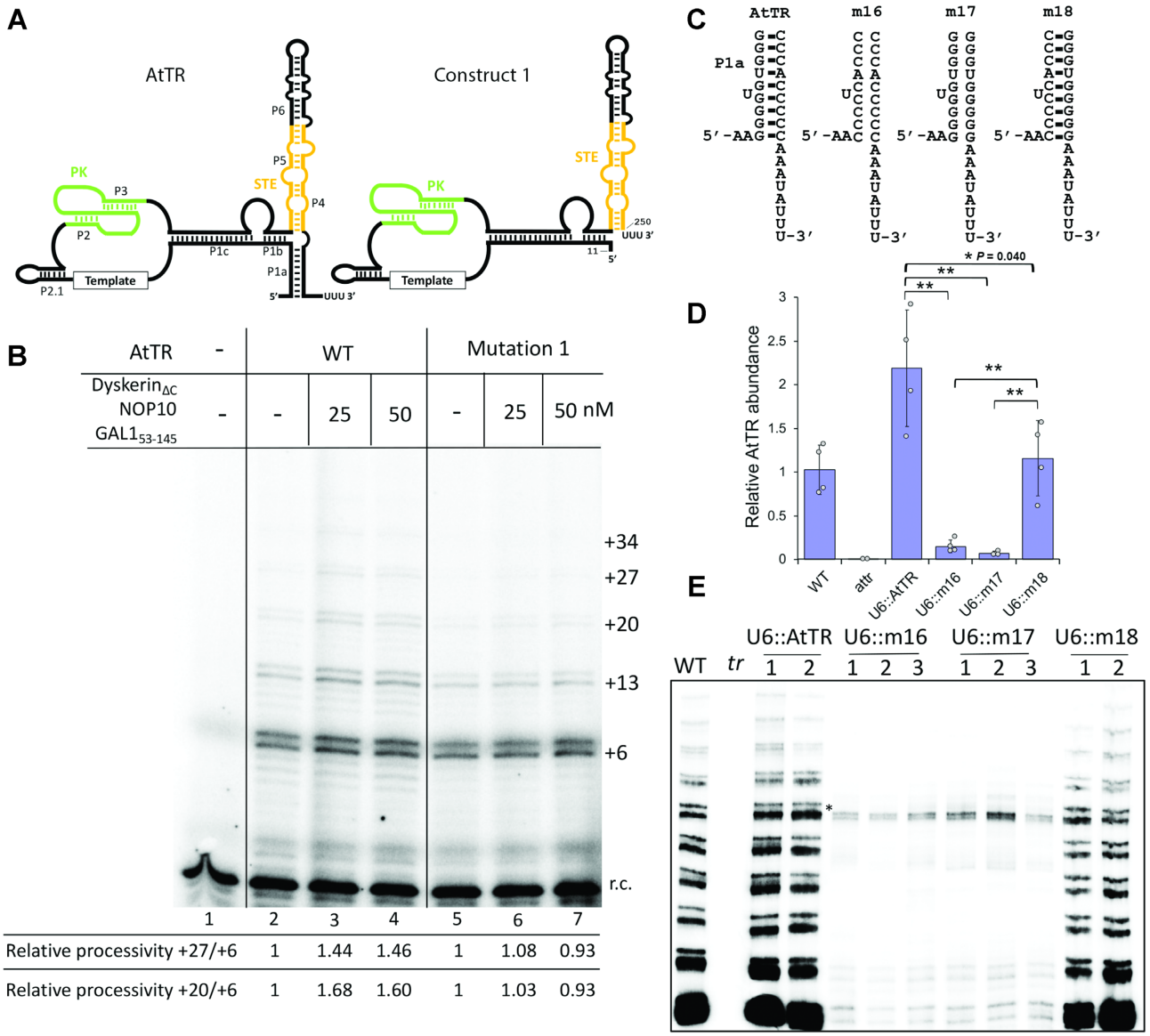

Figure 4. P1a is required for dyskerin stimulation of telomerase processivity *in vitro* and AtTR stability *in vivo*. (**A**) Secondary structures of WT AtTR and construct 1. (**B**) *In vitro* telomerase reconstitution assay with titration of Dyskerin$_{\Delta C}$-NOP10-GAL1$_{53-145}$ heterotrimer. WT AtTR or construct 1 was used independently as TR in this assay. Relative telomerase processivity is indicated at the bottom of the panel. Radiolabeled 18-mer recovery control (r.c.) was added before product purification and precipitation. (**C**) Schematic representation of WT AtTR and AtTR variants used for genetic complementation. (**D**) qPCR analysis of AtTR abundance in transgenic plants expressing WT AtTR or AtTR variants. A single data point represents an individual biological repeat. Error bars indicate standard deviation. $^{**}P$ value < 0.01 and $^{*}P$ value < 0.05 were calculated based on Student's *t*-test. (**E**) TRAP assay to measure telomerase activity in transgenic plants.

of telomerase RNP biogenesis and regulation. In this study, we investigated how two proteins implicated in vertebrate telomerase regulation and biogenesis engage the Arabidopsis telomerase RNP.

AtPOT1a is one of two *A. thaliana* orthologs of the human shelterin component, hPOT1 (45,46). We discovered that AtPOT1a physically binds TERT in an AtTR-independent manner, consistent with previous yeast two-hybrid and bimolecular fluorescence complementation data showing an interaction between AtPOT1a and residues 1–271 of TERT (46,61). Interestingly, this region of AtTERT is predicted to contain the TEN domain, the binding site for TPP1 to bridge the association of human POT1 and TERT (38,65). Since a TPP1 homolog has not been identified in Arabidopsis, these observations raise the possibility of a plant-specific TPP1-independent POT1a assembly on telomerase. Like hPOT1, AtPOT1a is not essential for TR accumulation *in vivo*, and its absence does not significantly impact AtTR structure. Intriguingly, however, residues within the alignment region of the telomere template are significantly more accessible in the absence of POT1a. These findings argue that the primary role of AtPOT1a, like the hPOT1-TPP1 heterodimer (43), is not to promote telomerase assembly, but rather to stimulate telomerase interaction with and extension of telomeric DNA (48,50).

Like POT1, dyskerin is highly conserved (66). Dyskerin has a strong binding preference for the H/ACA motif embedded within a subset of RNA Pol II transcribed snoRNAs found in yeast, vertebrates and plants, including Arabidopsis (67–69). The vertebrate dyskerin complex also associates with the H/ACA box within TR and is a stable component of the active telomerase RNP (25,28). Genetic (51) and biochemical data in *A. thaliana* and *A. cepa* (32,51) indicate that dyskerin contributes to telomerase function in plants. However, since AtTR and other plant TR molecules are expressed by RNA Pol III (13,32,33) and lack a canonical H/ACA motif, it has been unclear how dyskerin engages plant telomerase.

We addressed this conundrum by first confirming the dyskerin interaction with Arabidopsis telomerase and then demonstrating the interaction is dependent on AtTR. We report that dyskerin binds AtTR with high specificity and affinity and stimulates RAP of reconstituted telomerase *in vitro*. Unexpectedly, we found that dyskerin recognizes a plant-specific TWJ *in vitro* that is retained in all known plant TRs. This structure exhibits multiple base-pair covariations across different plant lineages, supporting its biological significance. Mammalian and yeast TR also maintain a TWJ, but it is constructed from local hairpins entirely embedded within the STE (also known as CR4/5). In contrast, the plant-specific TWJ is assembled by three independent RNA elements: the P4 stem from the STE, the P1b stem from the core-enclosing template boundary element, and the P1a stem. The mammalian TWJ interacts with TERT to promote telomerase RNP assembly (70). We hypothesize Arabidopsis TERT binds the corresponding region P5-P6 in AtTR, while the plant-specific TWJ is employed as a binding site for the dyskerin complex. The P1a stem is a critical element within the Arabidopsis TWJ, and we show it is important not only for dyskerin-mediated stimulation of telomerase RAP *in vitro* but also for AtTR stability and telomerase activity *in vivo*.

How Arabidopsis dyskerin came to bind a Pol III RNA that lacks an H/ACA motif is unclear, but a clue may be found in the history of TR regulation. The polymerase responsible for TR transcription has switched more than once during evolution (3). Since Arabidopsis harbors a variety of H/ACA snoRNA species (69), it is possible that dyskerin developed an alternative binding modality as it co-evolved with AtTR. In this view, AtTR may have originated as a Pol II transcript which then acquired an internal stretch of U-rich sequence downstream of the dyskerin binding site. This change, coupled with modification to the promoter, would be sufficient to enable Pol III-mediated transcription and termination, yet allow dyskerin binding to be retained.

There are several instances of telomerase-associated proteins that do not comply with canonical binding mechanisms. LaRP7 and other La family proteins are best known for their interaction with Pol III transcripts (71), and such factors include the telomerase subunits P43 in *Euplotes* and P65 in Tetrahymena (72–75). Intriguingly, the La-related protein family 7 (LaRP7) protein Pof8 is a constitutive subunit of *Schizosaccharomyces pombe* telomerase that directly binds the Pol II-transcribed SpTER1 (22,23). Although structural homology has been noted between Pof8 and P65 (21,76), Pof8 is reported to associate with PK of SpTER1 and play a key role in telomerase RNA folding quality control (76). Determining whether dyskerin serves as core component of *A. thaliana* telomerase or an accessory factor akin to Pof8 in fission yeast awaits a comprehensive understanding of plant telomerase RNP composition. Results of such studies may hold more surprises as AtTR was originally identified as a lncRNA responsive to hypoxia and salicylic acid (33), and has been implicated in the pathogen response (77). Thus, as suggested for vertebrate TR (78–81), Arabidopsis TR may assemble with different protein binding partners in different physiological contexts beyond the telomere realm.

DATA AVAILABILITY

MaPseq data generated in this project are available at NCBI (BioProject PRJNA721528).

SUPPLEMENTARY DATA

Supplementary Data are available at NAR Online.

ACKNOWLEDGEMENTS

We are grateful to Julian J.-L. Chen (Arizona State University) for helpful discussions and critical insights on the manuscript, for providing the pCITE-3xFLAG-AtTER plasmid used for reconstitution assays and for several RNA constructs tested in EMSA. We also thank Andrew Hillhouse (Genomics Core at the Texas A&M Institute for Genome Sciences and Society) for high-throughput sequencing support and Shippen lab members for thoughtful advice throughout this work.

FUNDING

National Science Foundation [MCB2047915, MCB1517817 to D.S.]. Funding for open access charge: National Science Foundation [MCB2047915].
Conflict of interest statement. None declared.

REFERENCES

1. Shay,J.W. and Wright,W.E. (2019) Telomeres and telomerase: three decades of progress. *Nat. Rev. Genet.*, **20**, 299–309.
2. Blackburn,E.H. and Collins,K. (2011) Telomerase: an RNP enzyme synthesizes DNA. *Cold Spring Harb. Perspect. Biol.*, **3**, a003558.
3. Podlevsky,J.D. and Chen,J.J. (2016) Evolutionary perspectives of telomerase RNA structure and function. *RNA Biol.*, **13**, 720–732.
4. Mitchell,J.R. and Collins,K. (2000) Human telomerase activation requires two independent interactions between telomerase RNA and telomerase reverse transcriptase. *Mol. Cell*, **6**, 361–371.
5. Qi,X., Li,Y., Honda,S., Hoffmann,S., Marz,M., Mosig,A., Podlevsky,J.D., Stadler,P.F., Selker,E.U. and Chen,J.J. (2013) The common ancestral core of vertebrate and fungal telomerase RNAs. *Nucleic Acids Res.*, **41**, 450–462.
6. Podlevsky,J.D., Li,Y. and Chen,J.J. (2016) The functional requirement of two structural domains within telomerase RNA emerged early in eukaryotes. *Nucleic Acids Res.*, **44**, 9891–9901.
7. Cash,D.D., Cohen-Zontag,O., Kim,N.K., Shefer,K., Brown,Y., Ulyanov,N.B., Tzfati,Y. and Feigon,J. (2013) Pyrimidine motif triple helix in the *Kluyveromyces lactis* telomerase RNA pseudoknot is essential for function in vivo. *Proc. Natl. Acad. Sci. U.S.A.*, **110**, 10970–10975.

8. Autexier,C. and Greider,C.W. (1998) Mutational analysis of the Tetrahymena telomerase RNA: identification of residues affecting telomerase activity in vitro. *Nucleic Acids Res.*, **26**, 787–795.
9. Gilley,D. and Blackburn,E.H. (1999) The telomerase RNA pseudoknot is critical for the stable assembly of a catalytically active ribonucleoprotein. *Proc. Natl. Acad. Sci. U.S.A.*, **96**, 6621–6625.
10. Brown,Y., Abraham,M., Pearl,S., Kabaha,M.M., Elboher,E. and Tzfati,Y. (2007) A critical three-way junction is conserved in budding yeast and vertebrate telomerase RNAs. *Nucleic Acids Res.*, **35**, 6280–6289.
11. Chen,J.L., Opperman,K.K. and Greider,C.W. (2002) A critical stem-loop structure in the CR4-CR5 domain of mammalian telomerase RNA. *Nucleic Acids Res.*, **30**, 592–597.
12. Mason,D.X., Goneska,E. and Greider,C.W. (2003) Stem-loop IV of tetrahymena telomerase RNA stimulates processivity in trans. *Mol. Cell. Biol.*, **23**, 5606–5613.
13. Song,J., Logeswaran,D., Castillo-Gonzalez,C., Li,Y., Bose,S., Aklilu,B.B., Ma,Z., Polkhovskiy,A., Chen,J.J. and Shippen,D.E. (2019) The conserved structure of plant telomerase RNA provides the missing link for an evolutionary pathway from ciliates to humans. *Proc. Natl. Acad. Sci. U.S.A.*, **116**, 24542–24550.
14. Egan,E.D. and Collins,K. (2012) Biogenesis of telomerase ribonucleoproteins. *RNA*, **18**, 1747–1759.
15. Akiyama,B.M., Loper,J., Najarro,K. and Stone,M.D. (2012) The C-terminal domain of *Tetrahymena thermophila* telomerase holoenzyme protein p65 induces multiple structural changes in telomerase RNA. *RNA*, **18**, 653–660.
16. Berman,A.J., Gooding,A.R. and Cech,T.R. (2010) Tetrahymena telomerase protein p65 induces conformational changes throughout telomerase RNA (TER) and rescues telomerase reverse transcriptase and TER assembly mutants. *Mol. Cell. Biol.*, **30**, 4965–4976.
17. Singh,M., Wang,Z., Koo,B.K., Patel,A., Cascio,D., Collins,K. and Feigon,J. (2012) Structural basis for telomerase RNA recognition and RNP assembly by the holoenzyme La family protein p65. *Mol. Cell*, **47**, 16–26.
18. Jiang,J., Chan,H., Cash,D.D., Miracco,E.J., Ogorzalek Loo,R.R., Upton,H.E., Cascio,D., O'Brien Johnson,R., Collins,K., Loo,J.A. *et al.* (2015) Structure of Tetrahymena telomerase reveals previously unknown subunits, functions, and interactions. *Science*, **350**, aab4070.
19. Box,J.A., Bunch,J.T., Tang,W. and Baumann,P. (2008) Spliceosomal cleavage generates the 3′ end of telomerase RNA. *Nature*, **456**, 910–914.
20. Noel,J.F., Larose,S., Abou Elela,S. and Wellinger,R.J. (2012) Budding yeast telomerase RNA transcription termination is dictated by the Nrd1/Nab3 non-coding RNA termination pathway. *Nucleic Acids Res.*, **40**, 5625–5636.
21. Basu,R., Eichhorn,C.D., Cheng,R., Peterson,R.D. and Feigon,J. (2020) Structure of S. pombe telomerase protein Pof8 C-terminal domain is an xRRM conserved among LARP7 proteins. *RNA Biol.*, **18**, 1181–1192.
22. Mennie,A.K., Moser,B.A. and Nakamura,T.M. (2018) LARP7-like protein Pof8 regulates telomerase assembly and poly(A)+TERRA expression in fission yeast. *Nat. Commun.*, **9**, 586.
23. Paez-Moscoso,D.J., Pan,L., Sigauke,R.F., Schroeder,M.R., Tang,W. and Baumann,P. (2018) Pof8 is a La-related protein and a constitutive component of telomerase in fission yeast. *Nat. Commun.*, **9**, 587.
24. Chen,J.L., Blasco,M.A. and Greider,C.W. (2000) Secondary structure of vertebrate telomerase RNA. *Cell*, **100**, 503–514.
25. Mitchell,J.R., Cheng,J. and Collins,K. (1999) A box H/ACA small nucleolar RNA-like domain at the human telomerase RNA 3′ end. *Mol. Cell. Biol.*, **19**, 567–576.
26. Zhu,Y., Tomlinson,R.L., Lukowiak,A.A., Terns,R.M. and Terns,M.P. (2004) Telomerase RNA accumulates in Cajal bodies in human cancer cells. *Mol. Biol. Cell*, **15**, 81–90.
27. Cristofari,G., Adolf,E., Reichenbach,P., Sikora,K., Terns,R.M., Terns,M.P. and Lingner,J. (2007) Human telomerase RNA accumulation in Cajal bodies facilitates telomerase recruitment to telomeres and telomere elongation. *Mol. Cell*, **27**, 882–889.
28. Tseng,C.K., Wang,H.F., Schroeder,M.R. and Baumann,P. (2018) The H/ACA complex disrupts triplex in hTR precursor to permit processing by RRP6 and PARN. *Nat. Commun.*, **9**, 5430.
29. Nguyen,T.H.D., Tam,J., Wu,R.A., Greber,B.J., Toso,D., Nogales,E. and Collins,K. (2018) Cryo-EM structure of substrate-bound human telomerase holoenzyme. *Nature*, **557**, 190–195.
30. Ghanim,G.E., Fountain,A.J., van Roon,A.M., Rangan,R., Das,R., Collins,K. and Nguyen,T.H.D. (2021) Structure of human telomerase holoenzyme with bound telomeric DNA. *Nature*, **593**, 449–453.
31. Nguyen,T.H.D., Collins,K. and Nogales,E. (2019) Telomerase structures and regulation: shedding light on the chromosome end. *Curr. Opin. Struct. Biol.*, **55**, 185–193.
32. Fajkus,P., Peska,V., Zavodnik,M., Fojtova,M., Fulneckova,J., Dobias,S., Kilar,A., Dvorackova,M., Zachova,D., Necasova,I. *et al.* (2019) Telomerase RNAs in land plants. *Nucleic Acids Res.*, **47**, 9842–9856.
33. Wu,J., Okada,T., Fukushima,T., Tsudzuki,T., Sugiura,M. and Yukawa,Y. (2012) A novel hypoxic stress-responsive long non-coding RNA transcribed by RNA polymerase III in Arabidopsis. *RNA Biol*, **9**, 302–313.
34. Baumann,P. and Price,C. (2010) Pot1 and telomere maintenance. *FEBS Lett.*, **584**, 3779–3784.
35. Lei,M., Podell,E.R. and Cech,T.R. (2004) Structure of human POT1 bound to telomeric single-stranded DNA provides a model for chromosome end-protection. *Nat. Struct. Mol. Biol.*, **11**, 1223–1229.
36. Baumann,P. and Cech,T.R. (2001) Pot1, the putative telomere end-binding protein in fission yeast and humans. *Science*, **292**, 1171–1175.
37. de Lange,T. (2018) Shelterin-mediated telomere protection. *Annu. Rev. Genet.*, **52**, 223–247.
38. Schmidt,J.C., Dalby,A.B. and Cech,T.R. (2014) Identification of human TERT elements necessary for telomerase recruitment to telomeres. *Elife*, **3**, e03563.
39. de Lange,T. (2005) Shelterin: the protein complex that shapes and safeguards human telomeres. *Genes Dev.*, **19**, 2100–2110.
40. Glousker,G., Briod,A.S., Quadroni,M. and Lingner,J. (2020) Human shelterin protein POT1 prevents severe telomere instability induced by homology-directed DNA repair. *EMBO J.*, **39**, e104500.
41. Loayza,D. and De Lange,T. (2003) POT1 as a terminal transducer of TRF1 telomere length control. *Nature*, **423**, 1013–1018.
42. Xu,M., Kiselar,J., Whited,T.L., Hernandez-Sanchez,W. and Taylor,D.J. (2019) POT1-TPP1 differentially regulates telomerase via POT1 His266 and as a function of single-stranded telomere DNA length. *Proc. Natl. Acad. Sci. U.S.A.*, **116**, 23527–23533.
43. Wang,F., Podell,E.R., Zaug,A.J., Yang,Y., Baciu,P., Cech,T.R. and Lei,M. (2007) The POT1-TPP1 telomere complex is a telomerase processivity factor. *Nature*, **445**, 506–510.
44. Latrick,C.M. and Cech,T.R. (2010) POT1-TPP1 enhances telomerase processivity by slowing primer dissociation and aiding translocation. *EMBO J.*, **29**, 924–933.
45. Shakirov,E.V., Surovtseva,Y.V., Osbun,N. and Shippen,D.E. (2005) The Arabidopsis Pot1 and Pot2 proteins function in telomere length homeostasis and chromosome end protection. *Mol. Cell. Biol.*, **25**, 7725–7733.
46. Rossignol,P., Collier,S., Bush,M., Shaw,P. and Doonan,J.H. (2007) Arabidopsis POT1A interacts with TERT-V(I8), an N-terminal splicing variant of telomerase. *J. Cell Sci.*, **120**, 3678–3687.
47. Beilstein,M.A., Renfrew,K.B., Song,X., Shakirov,E.V., Zanis,M.J. and Shippen,D.E. (2015) Evolution of the telomere-associated protein POT1a in *Arabidopsis thaliana* is characterized by positive selection to reinforce protein-protein interaction. *Mol. Biol. Evol.*, **32**, 1329–1341.
48. Surovtseva,Y.V., Shakirov,E.V., Vespa,L., Osbun,N., Song,X. and Shippen,D.E. (2007) Arabidopsis POT1 associates with the telomerase RNP and is required for telomere maintenance. *EMBO J.*, **26**, 3653–3661.
49. Renfrew,K.B., Song,X., Lee,J.R., Arora,A. and Shippen,D.E. (2014) POT1a and components of CST engage telomerase and regulate its activity in Arabidopsis. *PLoS Genet.*, **10**, e1004738.
50. Arora,A., Beilstein,M.A. and Shippen,D.E. (2016) Evolution of Arabidopsis protection of telomeres 1 alters nucleic acid recognition and telomerase regulation. *Nucleic Acids Res.*, **44**, 9821–9830.
51. Kannan,K., Nelson,A.D. and Shippen,D.E. (2008) Dyskerin is a component of the Arabidopsis telomerase RNP required for telomere maintenance. *Mol. Cell. Biol.*, **28**, 2332–2341.
52. Lermontova,I., Schubert,V., Bornke,F., Macas,J. and Schubert,I. (2007) Arabidopsis CBF5 interacts with the H/ACA snoRNP assembly factor NAF1. *Plant Mol. Biol.*, **65**, 615–626.
53. Fojtova,M., Peska,V., Dobsakova,Z., Mozgova,I., Fajkus,J. and Sykorova,E. (2011) Molecular analysis of T-DNA insertion mutants

identified putative regulatory elements in the AtTERT gene. *J. Exp. Bot.*, **62**, 5531–5545.
54. Zhang,X., Henriques,R., Lin,S.S., Niu,Q.W. and Chua,N.H. (2006) Agrobacterium-mediated transformation of *Arabidopsis thaliana* using the floral dip method. *Nat. Protoc.*, **1**, 641–646.
55. Iadevaia,V., Matia-Gonzalez,A.M. and Gerber,A.P. (2018) An oligonucleotide-based tandem RNA isolation procedure to recover eukaryotic mRNA-protein complexes. *J. Vis. Exp.*, **18**, 58223.
56. Chu,C., Quinn,J. and Chang,H.Y. (2012) Chromatin isolation by RNA purification (ChIRP). *J. Vis. Exp.*, **25**, 3912.
57. Wang,Z., Wang,M., Wang,T., Zhang,Y. and Zhang,X. (2019) Genome-wide probing RNA structure with the modified DMS-MaPseq in Arabidopsis. *Methods*, **155**, 30–40.
58. Chen,Y., Podlevsky,J.D., Logeswaran,D. and Chen,J.J. (2018) A single nucleotide incorporation step limits human telomerase repeat addition activity. *EMBO J.*, **37**, e97953.
59. Bose,S., Suescun,A.V., Song,J., Castillo-Gonzalez,C., Aklilu,B.B., Branham,E., Lynch,R. and Shippen,D.E. (2020) tRNA ADENOSINE DEAMINASE 3 is required for telomere maintenance in Arabidopsis thaliana. *Plant Cell Rep.*, **39**, 1669–1685.
60. Zappulla,D.C. and Cech,T.R. (2006) RNA as a flexible scaffold for proteins: yeast telomerase and beyond. *Cold Spring Harb. Symp. Quant. Biol.*, **71**, 217–224.
61. Majerska,J., Schrumpfova,P.P., Dokladal,L., Schorova,S., Stejskal,K., Oboril,M., Honys,D., Kozakova,L., Polanska,P.S. and Sykorova,E. (2017) Tandem affinity purification of AtTERT reveals putative interaction partners of plant telomerase in vivo. *Protoplasma*, **254**, 1547–1562.
62. Zubradt,M., Gupta,P., Persad,S., Lambowitz,A.M., Weissman,J.S. and Rouskin,S. (2017) DMS-MaPseq for genome-wide or targeted RNA structure probing in vivo. *Nat. Methods*, **14**, 75–82.
63. Hamma,T. and Ferre-D'Amare,A.R. (2010) The box H/ACA ribonucleoprotein complex: interplay of RNA and protein structures in post-transcriptional RNA modification. *J. Biol. Chem.*, **285**, 805–809.
64. Li,S., Duan,J., Li,D., Yang,B., Dong,M. and Ye,K. (2011) Reconstitution and structural analysis of the yeast box H/ACA RNA-guided pseudouridine synthase. *Genes Dev.*, **25**, 2409–2421.
65. Zaug,A.J., Podell,E.R., Nandakumar,J. and Cech,T.R. (2010) Functional interaction between telomere protein TPP1 and telomerase. *Genes Dev.*, **24**, 613–622.
66. Angrisani,A., Vicidomini,R., Turano,M. and Furia,M. (2014) Human dyskerin: beyond telomeres. *Biol. Chem.*, **395**, 593–610.
67. Balakin,A.G., Smith,L. and Fournier,M.J. (1996) The RNA world of the nucleolus: two major families of small RNAs defined by different box elements with related functions. *Cell*, **86**, 823–834.
68. Torchet,C., Badis,G., Devaux,F., Costanzo,G., Werner,M. and Jacquier,A. (2005) The complete set of H/ACA snoRNAs that guide rRNA pseudouridylations in *Saccharomyces cerevisiae*. *RNA*, **11**, 928–938.
69. Brown,J.W., Echeverria,M., Qu,L.H., Lowe,T.M., Bachellerie,J.P., Huttenhofer,A., Kastenmayer,J.P., Green,P.J., Shaw,P. and Marshall,D.F. (2003) Plant snoRNA database. *Nucleic Acids Res.*, **31**, 432–435.
70. Bley,C.J., Qi,X., Rand,D.P., Borges,C.R., Nelson,R.W. and Chen,J.J. (2011) RNA-protein binding interface in the telomerase ribonucleoprotein. *Proc. Natl. Acad. Sci. U.S.A.*, **108**, 20333–20338.
71. Bousquet-Antonelli,C. and Deragon,J.M. (2009) A comprehensive analysis of the La-motif protein superfamily. *RNA*, **15**, 750–764.
72. Witkin,K.L. and Collins,K. (2004) Holoenzyme proteins required for the physiological assembly and activity of telomerase. *Genes Dev.*, **18**, 1107–1118.
73. Min,B. and Collins,K. (2009) An RPA-related sequence-specific DNA-binding subunit of telomerase holoenzyme is required for elongation processivity and telomere maintenance. *Mol. Cell*, **36**, 609–619.
74. Aigner,S., Lingner,J., Goodrich,K.J., Grosshans,C.A., Shevchenko,A., Mann,M. and Cech,T.R. (2000) Euplotes telomerase contains an La motif protein produced by apparent translational frameshifting. *EMBO J.*, **19**, 6230–6239.
75. Aigner,S., Postberg,J., Lipps,H.J. and Cech,T.R. (2003) The Euplotes La motif protein p43 has properties of a telomerase-specific subunit. *Biochemistry*, **42**, 5736–5747.
76. Hu,X., Kim,J.K., Yu,C., Jun,H.I., Liu,J., Sankaran,B., Huang,L. and Qiao,F. (2020) Quality-control mechanism for telomerase RNA folding in the cell. *Cell Rep.*, **33**, 108568.
77. Li,S., Nayar,S., Jia,H., Kapoor,S., Wu,J. and Yukawa,Y. (2020) The Arabidopsis hypoxia inducible AtR8 long non-coding RNA also contributes to plant defense and root elongation coordinating with WRKY genes under low levels of salicylic acid. *Noncoding RNA*, **6**, 8.
78. Ting,N.S., Pohorelic,B., Yu,Y., Lees-Miller,S.P. and Beattie,T.L. (2009) The human telomerase RNA component, hTR, activates the DNA-dependent protein kinase to phosphorylate heterogeneous nuclear ribonucleoprotein A1. *Nucleic Acids Res.*, **37**, 6105–6115.
79. Kedde,M., le Sage,C., Duursma,A., Zlotorynski,E., van Leeuwen,B., Nijkamp,W., Beijersbergen,R. and Agami,R. (2006) Telomerase-independent regulation of ATR by human telomerase RNA. *J. Biol. Chem.*, **281**, 40503–40514.
80. Raghunandan,M., Geelen,D., Majerova,E. and Decottignies,A. (2021) NHP2 downregulation counteracts hTR-mediated activation of the DNA damage response at ALT telomeres. *EMBO J.*, **40**, e106336.
81. Gazzaniga,F.S. and Blackburn,E.H. (2014) An antiapoptotic role for telomerase RNA in human immune cells independent of telomere integrity or telomerase enzymatic activity. *Blood*, **124**, 3675–3684.